

## Microscopic Analysis of Elastic and Inelastic $\pi$ -Nucleus Scattering at Energies of (3 3) Resonance

**E.V. Zemlyanaya**<sup>1,2</sup>, **V.K. Lukyanov**<sup>1</sup>, **K.V. Lukyanov**<sup>1,2</sup>,  
**I.A.M. Abdul-Magead**<sup>3</sup>, **E.I. Zhabitskaya**<sup>1,2</sup>, **M.V. Zhabitsky**<sup>1</sup>

<sup>1</sup>Joint Institute for Nuclear Research, 141980 Dubna, Russia

<sup>2</sup>State University "Dubna", 141980 Dubna, Russia

<sup>3</sup>Cairo University, Cairo, Giza, Egypt

**Abstract.** The microscopic model of optical potential (OP) is applied for calculations of the  $\pi^\pm$  scattering on the nuclei  $^{28}\text{Si}$ ,  $^{58}\text{Ni}$ ,  $^{40}\text{Ca}$ ,  $^{208}\text{Pb}$  at energies 162, 180, and 291 MeV. Such OP depends on the nuclear density distributions and parameters of the  $\pi N$  scattering amplitudes which are fitted to the pion-nucleus elastic cross sections. Also, calculations are made using the Kisslinger-type and Wood-Saxon potentials, and they are found to be in well agreement to those obtained with a help of our OPs. Then the  $\pi N$  parameters are utilized for inelastic scattering with excitations of the  $2^+$  and  $3^-$  collective states. The only adjusted parameters are the quadrupole  $\beta_2$  or octupole  $\beta_3$  deformations of nuclei. The cross sections of elastic and inelastic scattering are calculated with help of computer code DWUCK4 by solving the relativistic wave equation, and thus the relativistic and distortion effects in initial and final channels of the process are accounted for exactly. The calculated cross sections have been found to be in a fairly well agreement with the corresponding experimental data. The role of the nuclear in-medium effect on the  $\pi N$ -scattering amplitude is discussed.

### 1 Introduction

Two approaches are usually employed in theoretical study of  $\pi$ -nucleus scattering. *First*, microscopic local transformed Kisslinger potential having 12 fitted parameters [1]. It is based on  $s$ - and  $p$ -  $\pi N$  scattering amplitudes and respective density distribution function of nuclei. *Second*, the Glauber high-energy approximation (HEA) for the  $\pi$ -nucleus amplitude that uses in eikonal phase an analytic form of the  $\pi N$  amplitude and the nuclear density integrated along the straight line trajectory of scattering [2].

Our approach is based on construction of the HEA-based folding  $\pi$ -nucleus microscopic optical potential (OP) [3] which is applied for calculation of pion-nucleus differential cross-sections by solving the relativistic wave equation [4]. Our aim is an explanation of experimental data on both elastic and inelastic

scattering in the region of  $\pi N$  ( $3\ 3$ )-resonance energies and estimation of “in-medium” effect on the elementary  $\pi$ -nucleon amplitude.

The  $\pi N$  amplitude depends on three parameters: total cross section  $\sigma$ , the ratio  $\alpha$  of real to imaginary part of the forward  $\pi N$  amplitude, and the slope parameter  $\beta$  [4]. They are obtained by fitting the calculated  $\pi A$  differential cross sections to the respective experimental data on *elastic* scattering

The established best-fit “in-medium”  $\pi N$  parameters are compared with these for the corresponding “free”  $\pi N$  scattering amplitudes.

Then, the best-fit “in-medium”  $\pi N$  parameters are used for analysis of inelastic scattering data. But for inelastic scattering, we substitute into the microscopic OP the generalized density distribution function  $\rho(r, \xi)$  depended on collective variables  $\xi$  of a target nucleus. Thus one can obtain the microscopic transition OP (TOP)  $U_{inel}(\mathbf{r}, \xi)$  responsible for inelastic scattering with excitations of the nuclear collective states [5]. This TOP provides calculations of the pion-nucleus inelastic scattering with excitations of the quadruple  $2^+$  and octuple  $3^-$  collective states of the target nuclei studied earlier in elastic scattering of pions. This scheme does not contain free parameters except the static (or dynamic) deformations of nuclei  $\beta_\lambda$  ( $\lambda = 2, 3$ ) that characterize their excited states.

Application is presented for elastic and inelastic scattering of pions on nuclei  $^{28}\text{Si}$ ,  $^{58}\text{Ni}$ ,  $^{40}\text{Ca}$  and  $^{208}\text{Pb}$  at energies 162, 180, and 291 MeV. Experimental data are from [6–8].

## 2 Elastic Scattering

### 2.1 Basic equations

The differential cross sections are calculated as done in [9] by solving the relativistic wave equation with the help of the standard DWUCK4 computer code [10]:

$$(\Delta + k^2) \psi(\vec{r}) = 2\bar{\mu}U(r)\psi(\vec{r}), \quad U(r) = U^H(r) + U_C(r) \quad (1)$$

Here  $k$  is relativistic momentum of pions in c.m. system,

$$k = \frac{M_A k^{\text{lab}}}{\sqrt{(M_A + m_\pi)^2 + 2M_A T^{\text{lab}}}}, \quad k^{\text{lab}} = \sqrt{T^{\text{lab}}(T^{\text{lab}} + 2m_\pi)},$$

$\bar{\mu} = \frac{EM_A}{E + M_A}$  – relativistic reduced mass,  $E = \sqrt{k^2 + m_\pi^2}$  – total energy,  $m_\pi$  and  $M_A$  – the pion and nucleus masses.

HEA-based microscopic OP for elastic scattering has the form [3]:

$$U^H = -\sigma(\alpha + i) \cdot \frac{\hbar c \beta_c}{(2\pi)^2} \int_0^\infty dq q^2 j_0(qr) \rho(q) f_\pi(q), \quad (2)$$

where  $f_\pi(q)$  is formfactor of the  $\pi N$ -scattering amplitude:

$$F_{\pi N}(q) = \frac{k}{4\pi} \sigma[i + \alpha] \cdot f_\pi(q), \quad f_\pi(q) = e^{-\beta q^2/2}, \quad (3)$$

$\hbar c = 197.327$  MeV·fm,  $j_0$  is the spherical Bessel function,  $\beta_c = k/E$ ,  $\sigma$  – total cross section of  $\pi N$  scattering,  $\alpha$  – ratio of real to imaginary part of the forward  $\pi N$  amplitude,  $\beta$  – the slope parameter,  $\rho(q)$  – form factor of the nuclear density distribution taken as the symmetrized Fermi-function:

$$\rho_{SF}(r) = \rho_0 \frac{\sinh(R/a)}{\cosh(R/a) + \cosh(r/a)}, \quad \rho_0 = \frac{A}{1.25\pi R^3} \left[1 + \left(\frac{\pi a}{R}\right)^2\right]^{-1}. \quad (4)$$

The radius  $R$  and diffuseness  $a$  are known from electron-nucleus scattering data.

The charge-independent principle  $f_{\pi^\pm p} = f_{\pi^\mp n}$  lets to use only 3 averaged parameters for  $\pi N$ -amplitude instead of 12 for  $\pi^\pm p$  and  $\pi^\pm n$ , separately. So, three “in-medium” parameters  $\sigma$ ,  $\alpha$ ,  $\beta$  of the  $\pi N$  scattering amplitude are obtained by fitting to the experimental  $\pi A$  differential cross sections. In order to obtain these parameters, we minimize the function

$$\chi^2 = f(\sigma, \alpha, \beta) = \sum_i \frac{(y_i - \hat{y}_i(\sigma, \alpha, \beta))^2}{s_i^2}, \quad (5)$$

where  $y_i = \frac{d\sigma}{d\Omega}$  and  $\hat{y}_i = \frac{d\sigma}{d\Omega}(\sigma, \alpha, \beta)$  are, respectively, experimental and theoretical differential cross sections,  $s_i$  – experimental errors. The fitting procedure is based on the asynchronous differential evolution algorithm [11].

## 2.2 Results of calculations

Figures 1 and 2 demonstrate a reasonable agreement of the calculated and experimental differential cross sections of elastic pion-nucleus scattering at energies 291 and 162 MeV. Experimental data in Figures 1 and 2 are, respectively, from [6] and [7]. In calculations, radius  $R$  and diffuseness  $a$  of the target nuclear density distribution are following:  $R = 3.134$  fm and  $a = 0.477$  fm for  $^{28}\text{Si}$  [12],  $R = 4.2$  fm and  $a = 0.475$  fm for  $^{58}\text{Ni}$  [13],  $R = 6.654$  fm and  $a = 0.475$  fm for  $^{208}\text{Pb}$  [14]. Parameters  $\alpha$ ,  $\beta$ ,  $\sigma$  of “in-medium”  $\pi N$  amplitude are given in [4]. More calculations (for the energies 130, 226, and 230 MeV) are presented in [4].

Figure 3 demonstrates the case of elastic scattering  $\pi^+$  cross sections on  $^{58}\text{Ni}$  at 162 MeV, calculated using the 3-parameter microscopic OP (2) in comparison with results for the 12-parameter local Kisslinger-Ericson  $\pi A$ -potential calculated as follows

$$U_{KE}(r) = \frac{(\hbar c)^2}{2\omega} \left\{ \frac{q(r)}{1 - \alpha(r)} - \frac{k^2 \alpha(r)}{1 - \alpha(r)} - \left[ \frac{0.5 \nabla^2 \alpha(r)}{1 - \alpha(r)} + \left( \frac{0.5 \nabla \alpha(r)}{1 - \alpha(r)} \right)^2 \right] \right\} \quad (6)$$

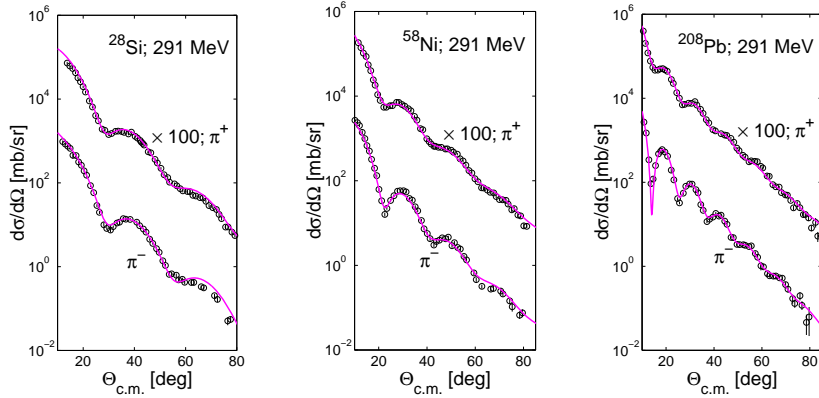


Figure 1. Comparison of the calculated pion-nucleus elastic scattering differential cross sections at  $T^{\text{lab}} = 291$  MeV with experimental data from [6]. The best-fit “in-medium” parameters  $\sigma$ ,  $\alpha$ , and  $\beta$  are given in [4].

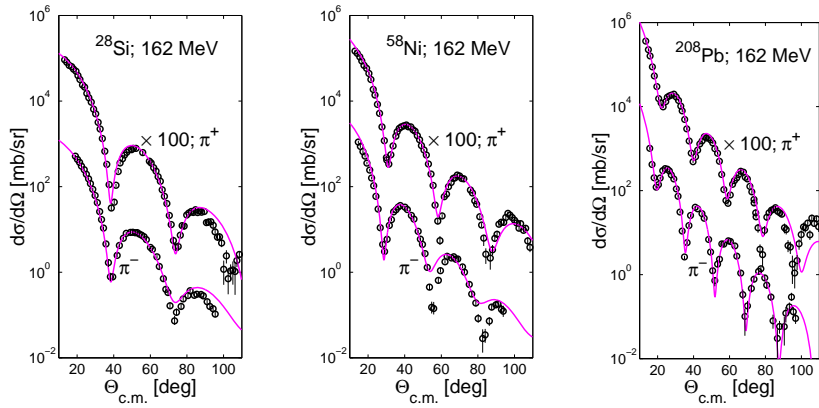


Figure 2. The same as in Figure 1 but for  $T^{\text{lab}} = 162$  MeV. The experimental data are from [7].

where  $\omega$  is the total pion energy;  $q(r)$  and  $\alpha(r)$  are the nuclear density dependent functions parameterized in [1]. Parameters of the  $\pi N$  amplitude (3) in microscopic OP are following:  $\alpha = 0.44$ ,  $\beta = 0.75$  fm,  $\sigma = 9.28$  fm.

It is seen that both approaches provide almost the same agreement of calculated cross sections with experimental data in spite the very different shape of potential curves.

Comparison of microscopic OP (2) with the standard Woods-Saxon (WS) potential in case  $\pi^- + {}^{208}\text{Pb}$  at 162 MeV is presented in Figure 4. Parameters of 6-parameter WS potential have been taken from [15]:

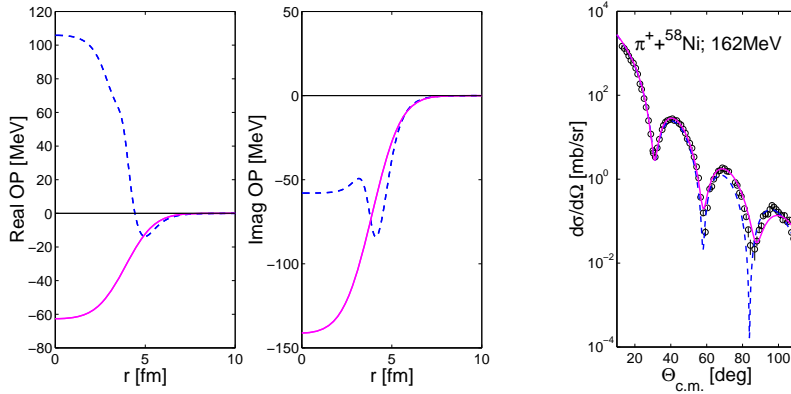


Figure 3. Solid: 3-parameter microscopic OP (2) and respective differential cross sections of elastic scattering  $\pi^+$  on  $^{58}\text{Ni}$  at 162 MeV. Dashed: the same for the 12-parameter Kisslinger potential (6). Experimental data from [7].

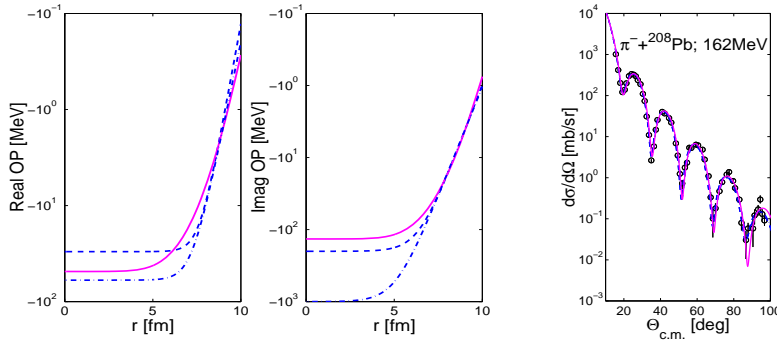


Figure 4. Solid: 3-parameter microscopic OP (2) and respective differential cross sections of elastic scattering  $\pi^-$  +  $^{208}\text{Pb}$  at 162 MeV. Dashed and dash-dotted: the same for the 6-parameter WS potential, parameters are given in the text. Experimental data from [7].

1.  $V_0 = -30.15\text{MeV}$ ,  $a_v = 0.431\text{ fm}$ ,  $R_v = 7.649\text{ fm}$ ,  $W_0 = -200\text{ MeV}$ ,  
 $a_w = 0.675\text{ fm}$ ,  $R_w = 6.408\text{ fm}$  (dashed lines in Figure 4)
2.  $V_0 = -59.7\text{ MeV}$ ,  $a_v = 0.489\text{ fm}$ ,  $R_v = 7.210\text{ fm}$ ,  $W_0 = -100\text{ MeV}$ ,  
 $a_w = 0.715\text{ fm}$ ,  $R_w = 5.091\text{ fm}$  (dash-dotted lines in Figure 4)

Both sets of parameters are found to provide the same agreement with experimental data ( $\chi^2 = 2.2$ ) and almost the same quantity of reaction cross section ( $\sigma_R = 2690\text{ mb}$  and  $\sigma_R = 2707\text{ mb}$ , respectively, for the 1st and the 2nd set of parameters).

The microscopic OP in Figure 4 was calculated with  $\alpha = 0.34$ ,  $\beta = 1.02\text{ fm}$ ,  $\sigma = 9.69\text{ fm}$ . We obtained the  $\pi N$  total reaction cross section  $\sigma_R = 2624\text{ mb}$  and deviation (5)  $\chi^2 = 3.7$ . Respective potentials and cross sections are shown

in Figure 4 by solid lines. It is seen that the potentials have the very different strength but they are very close in the peripheral region of target nucleus. It looks, this region is most important for explanation of experimental data.

One can conclude that our approach based on 3-parameter OP, allows one to explain experimental data on pion-nucleus elastic scattering. Agreement between theoretical and experimental cross sections is comparable with results of application of 12-parameter Kisslinger potential (6) and 6-parameter standard WS potential.

### 3 Inelastic Scattering

#### 3.1 Basic equations

In the inelastic scattering case, as in Section 2, we utilize the HEA-based microscopic OP but in the generalized form [16]:

$$U_{\text{opt}}(r) = -\frac{(\hbar c)\beta_c}{2(2\pi)^3} \sigma [i + \alpha] \cdot \int e^{-i\mathbf{q}\mathbf{r}} \rho(\mathbf{q}) f_\pi(q) q^2 dq, \quad \beta_c = k/E \quad (7)$$

where  $\rho(q)$  – formfactor of a nuclear density distribution and  $f_\pi(q)$  – formfactor of  $\pi N$ -amplitude as done in (3). To get the generalized microscopic OP for calculating both elastic and inelastic scattering, we use the generalized form factor of a density distribution function

$$\rho(\mathbf{q}) = \int e^{i\mathbf{q}\mathbf{r}} \rho(\mathbf{r}(\xi)) d^3r \quad (8)$$

where  $\mathbf{r}(\xi)$  includes a dependence on the  $\xi$ -variables that define collective motion of a nucleons. We use the following standard prescription:

$$\mathbf{r} \Rightarrow r + \delta^{(\lambda)}(\mathbf{r}), \quad \delta^{(\lambda)}(\mathbf{r}) = -r \left(\frac{r}{R}\right)^{\lambda-2} \sum_{\mu} \alpha_{\lambda\mu} Y_{\lambda\mu}(\hat{r}), \quad (9)$$

where  $\alpha_{\lambda\mu}$  are the nuclear quadrupole and octupole deformation collective variables for  $\lambda=2,3$ .

Substituting this one in the density and then in the initial optical potential, and terminating their expansions at linear terms in  $\delta^{(\lambda)}(\mathbf{r})$  one obtains

$$\rho(\mathbf{r}) = \rho(r) + \rho_\lambda(r) \sum_{\mu} \alpha_{\lambda\mu} Y_{\lambda\mu}(\hat{r}), \quad \rho_\lambda(r) = -r \left(\frac{r}{R}\right)^{\lambda-2} \frac{d\rho(r)}{dr} \quad (10)$$

and then one gets their form factors

$$\rho(\mathbf{q}) = \rho(q) + \rho_\lambda(q) i^\lambda \sum_{\mu} \alpha_{\lambda\mu} Y_{\lambda\mu}(\hat{q}), \quad (11)$$

$$\rho(q) = 4\pi \int j_0(qr) \rho(r) r^2 dr, \quad (12)$$

$$\rho_\lambda(q) = 4\pi \int j_\lambda(qr) \rho_\lambda(r) r^2 dr. \quad (13)$$

Finally, we obtain potentials for elastic and inelastic scattering:

$$U(\mathbf{r}) = U_{\text{opt}}(r) + U^{(\lambda)}(\mathbf{r}), \quad U^{(\lambda)}(\mathbf{r}) = U_{\lambda}(r) \sum_{\mu} \alpha_{\lambda\mu} Y_{\lambda\mu}(\hat{r}), \quad (14)$$

$$U_{\text{opt}}(r) = -\frac{(\hbar c)\beta_c}{(2\pi)^2} \sigma (\alpha + i) \int j_0(qr) \rho(q) f_{\pi}(q) q^2 dq, \quad (15)$$

$$U_{\lambda}(r) = -\frac{(\hbar c)\beta_c}{(2\pi)^2} \sigma (\alpha + i) \int j_{\lambda}(qr) \rho_{\lambda}(q) f_{\pi}(q) q^2 dq. \quad (16)$$

Here the spherically symmetric part  $U_{\text{opt}}(r)$  provides elastic scattering calculations while the  $U_{\lambda}(r)$  is the transition OP used for calculations of inelastic scattering cross sections with excitations of the  $2^+$  and  $3^-$  collective states of nuclei.

### 3.2 Results of calculations

Elastic and inelastic scattering cross sections in cases  $\pi^{\pm} + {}^{58}\text{Ni}$  at 162 MeV,  $\pi^{\pm} + {}^{40}\text{Ca}$  at 180 MeV, and  $\pi^{\pm} + {}^{58}\text{Ni}$  at 291 MeV are presented, respectively, in Figures 5, 6, and 7. Solid curves have been calculated on the basis of our

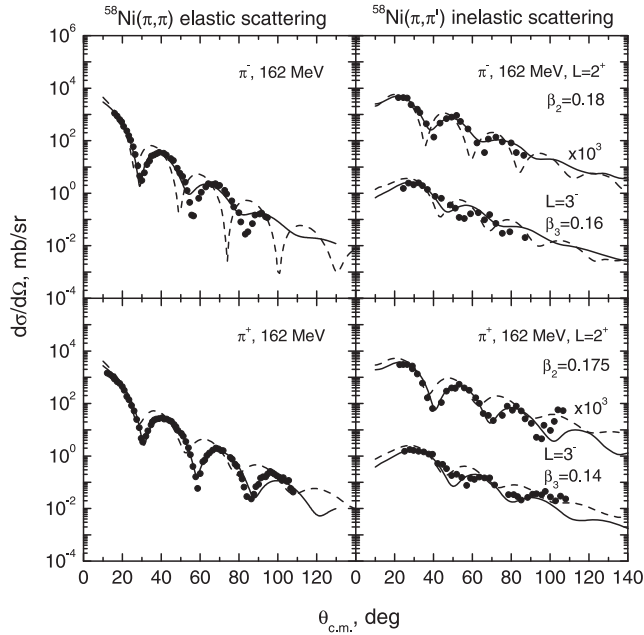


Figure 5. Elastic (left panel) and inelastic (right panel) scattering cross sections in case  $\pi^{\pm} + {}^{58}\text{Ni}$  at 162 MeV. Solid: calculation with "in-medium"  $\pi N$  parameters  $\alpha$ ,  $\beta$ ,  $\sigma$  from [4]; dashed: calculation with "free"  $\pi N$  parameters from [17]. Experimental data from [7].

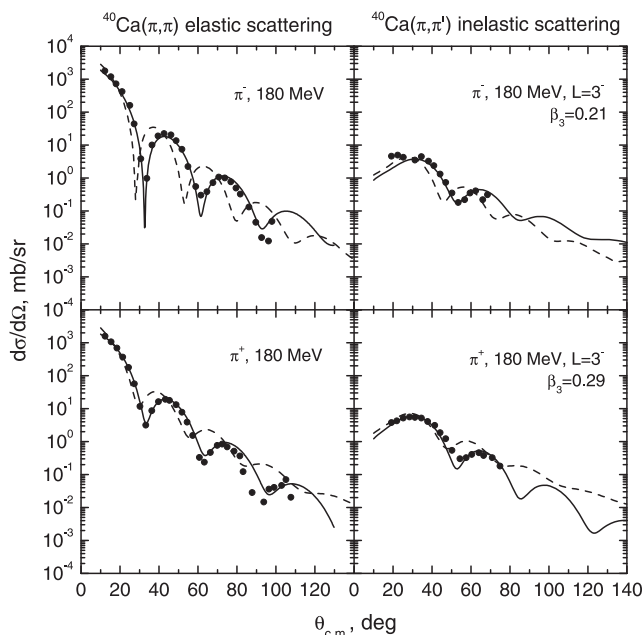


Figure 6. The same as in Figure 5 but for  $\pi^\pm + {}^{40}\text{Ca}$  at 180 MeV. Experimental data from [8].

microscopic approach with “in-medium” parameters  $\alpha$ ,  $\beta$ ,  $\sigma$  from [4] and with parameter of deformation fitted to experimental data on inelastic scattering [5]. Experimental data in Figures 5, 6, 7 are, respectively, from [7], [8], and [6]. Dashed curves are the calculations with the parameters  $\sigma$ ,  $\alpha$ ,  $\beta$  that correspond to the pion scattering on “free” nucleons at respective energies [17]. More calculations are presented in our recent paper [16].

It is seen that “free”  $\pi N$  parameters  $\alpha$ ,  $\beta$ ,  $\sigma$  cannot explain experimental data for the intermediate energies, in particular, 162 MeV and 180 MeV (Figures 5 and 6). Contrary, in the case of 291 MeV out of the (3 3) resonance, the “in-medium” and “free” curves are close between other, see Figure 7. This can mean that in-medium effect is strong at the energies of maximum of (3 3) resonance (between 150 and 200 MeV) and it becomes weak as  $T^{\text{lab}} > 250$  MeV. This is confirmed by comparison of averaged “in-medium” and “free” parameters  $\sigma$ ,  $\alpha$ ,  $\beta$  of  $\pi N$  scattering amplitude, see [4].

#### 4 Summary

- The HEA-based 3-parametric microscopic OP is shown to provide a reasonable agreement with experimental data of  $\pi^\pm$ -nucleus elastic and inelastic scattering at energies of (3 3) resonance.

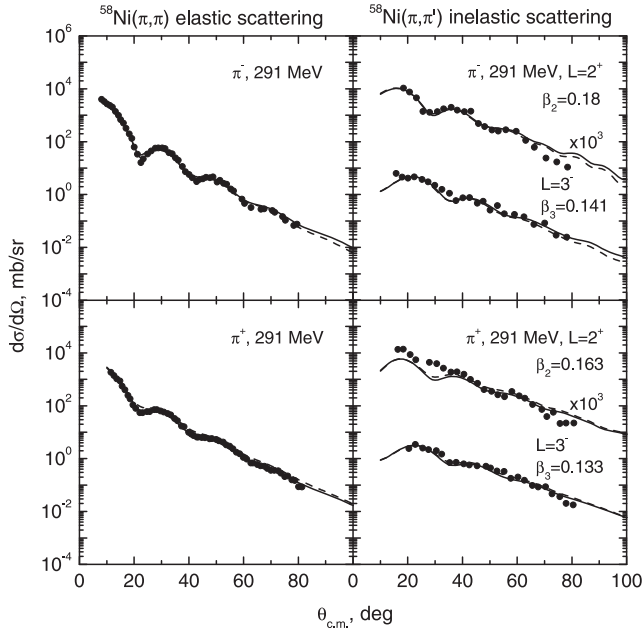


Figure 7. The same as in Figure 5 but for  $\pi^\pm + {}^{40}\text{Ca}$  at 180 MeV. Experimental data from [6].

- In the case of inelastic scattering, the proposed approach operates with the primary nature of a target nucleus: *the density distribution function*, while the other models use the secondary description function – a derivative of *an optical potential* of scattering.
- If one so explains elastic scattering then the only structure parameter, the deformation of a target nucleus  $\beta_\lambda$  is necessary to fit the data on inelastic scattering. The forms of theoretical curves are not to be fitted in such comparisons with the data.

The work is supported by the Program of cooperation between JINR and Egypt.

## References

- [1] M.B. Johnson and G.R. Satchler, *Ann. Phys.* **248** (1996) 134.
- [2] R.J. Glauber, *Lectures in Theoretical Physics*, (New York: Interscience, 1959) 315.
- [3] V.K. Lukyanov, E.V. Zemlyanaya, K.V. Lukyanov, *Phys. At. Nucl.* **69** (2006) 240.
- [4] V.K. Lukyanov, E.V. Zemlyanaya, K.V. Lukyanov, E.I. Zhabitskaya, and M.V. Zhabitsky, *Phys. At. Nucl.* **77** (2014) 100.
- [5] V.K. Lukyanov, E.V. Zemlyanaya, K.V. Lukyanov, A.Y. Ellithi, and I.A.M. Abdul-Magead, *Int. J. Mod. Phys. E* **24** (2015) 1550035.

- [6] D.F. Geesaman *et al.*, *Phys. Rev. C* **23** (1981) 2635.
- [7] C. Olmer *et al.*, *Phys. Rev. C* **21** (1980) 254.
- [8] P. Gretillat *et al.*, *Nucl. Phys. A* **364** (1981) 270-284.
- [9] V.K. Lukyanov, E.V. Zemlyanaya, K.V. Lukyanov, and K.M. Hanna, *Phys. At. Nucl.* **73** (2010) 1443.
- [10] P.D. Kunz and E. Rost, in *Computational Nuclear Physics*, Vol.2, Eds. Langanke K. et al., (Springer-Verlag, 1993) 88.
- [11] E. Zhabitskaya, M. Zhabitsky. *Lect. Notes Comput. Sci.* **7125** (2012) 328.
- [12] V.K. Lukyanov, E.V. Zemlyanaya, B. Słowinski, *Phys. At. Nucl.* **67** (2004) 1282.
- [13] M. El-Azab, G.R. Satchler, *Nucl. Phys. A* **438** (1985) 525.
- [14] J.D. Patterson, R.J. Peterson, *Nucl. Phys. A* **717** (2003) 235.
- [15] G.R. Satchler, *Nucl. Phys. A* **540** (1992) 533.
- [16] V.K. Lukyanov, E.V. Zemlyanaya, K.V. Lukyanov, and I.A.M. Abdul-Magead, *Phys. At. Nucl.* **79** (2016); in press.
- [17] M.P. Locher *et al.*, *Nucl. Phys. B* **27** (1971) 598.